

See discussions, stats, and author profiles for this publication at: <https://www.researchgate.net/publication/11616085>

Synthetic and Structural Studies on $[\text{Fe}_2(\text{SR})_2(\text{CN})_x(\text{CO})_{6-x}]_x$ - as Active Site Models for Fe-Only Hydrogenases

ARTICLE in JOURNAL OF THE AMERICAN CHEMICAL SOCIETY · JANUARY 2002

Impact Factor: 12.11 · DOI: 10.1021/ja016071v · Source: PubMed

CITATIONS

214

READS

35

5 AUTHORS, INCLUDING:



Frederic Gloaguen

CNRS, UBO Brest

81 PUBLICATIONS 3,890 CITATIONS

SEE PROFILE



Scott R Wilson

University of Illinois, Urbana-Champaign

389 PUBLICATIONS 11,594 CITATIONS

SEE PROFILE

Synthetic and Structural Studies on $[\text{Fe}_2(\text{SR})_2(\text{CN})_x(\text{CO})_{6-x}]^{x-}$ as Active Site Models for Fe-Only Hydrogenases

Frédéric Gloaguen, Joshua D. Lawrence, Michael Schmidt, Scott R. Wilson, and Thomas B. Rauchfuss*

Contribution from the Department of Chemistry, University of Illinois at Urbana-Champaign, Urbana, Illinois 61801

Received April 24, 2001

Abstract: A series of models for the active site (H-cluster) of the iron-only hydrogenase enzymes (Fe-only H_2 -ases) were prepared. Treatment of MeCN solutions of $\text{Fe}_2(\text{SR})_2(\text{CO})_6$ with 2 equiv of Et_4NCN gave $[\text{Fe}_2(\text{SR})_2(\text{CN})_2(\text{CO})_4]^{2-}$ compounds. IR spectra of the dicyanides feature four ν_{CO} bands between 1965 and 1870 cm^{-1} and two ν_{CN} bands at 2077 and 2033 cm^{-1} . For alkyl derivatives, both diequatorial and axial-equatorial isomers were observed by NMR analysis. Also prepared were a series of dithiolate derivatives $(\text{Et}_4\text{N})_2[\text{Fe}_2(\text{SR})_2(\text{CN})_2(\text{CO})_4]$, where $(\text{SR})_2 = \text{S}(\text{CH}_2)_2\text{S}$, $\text{S}(\text{CH}_2)_3\text{S}$. Reaction of Et_4NCN with $\text{Fe}_2(\text{S}-t\text{-Bu})_2(\text{CO})_6$ gave initially $[\text{Fe}_2(\text{S}-t\text{-Bu})_2(\text{CN})_2(\text{CO})_4]^{2-}$, which comproporportionated to give $[\text{Fe}_2(\text{S}-t\text{-Bu})_2(\text{CN})(\text{CO})_5]^-$. The mechanism of the CN^- -for- CO substitution was probed as follows: (i) excess CN^- with a 1:1 mixture of $\text{Fe}_2(\text{SMe})_2(\text{CO})_6$ and $\text{Fe}_2(\text{SC}_6\text{H}_4\text{Me})_2(\text{CO})_6$ gave no mixed thiolates, (ii) treatment of $\text{Fe}_2(\text{S}_2\text{C}_3\text{H}_6)(\text{CO})_6$ with Me_3NO followed by Et_4NCN gave $(\text{Et}_4\text{N})[\text{Fe}_2(\text{S}_2\text{C}_3\text{H}_6)(\text{CN})(\text{CO})_5]$, which is a well-behaved salt, (iii) treatment of $\text{Fe}_2(\text{S}_2\text{C}_3\text{H}_6)(\text{CO})_6$ with Et_4NCN in the presence of excess PMe_3 gave $(\text{Et}_4\text{N})[\text{Fe}_2(\text{S}_2\text{C}_3\text{H}_6)(\text{CN})(\text{CO})_4(\text{PMe}_3)]$ much more rapidly than the reaction of PMe_3 with $(\text{Et}_4\text{N})[\text{Fe}_2(\text{S}_2\text{C}_3\text{H}_6)(\text{CN})(\text{CO})_5]$, and (iv) a competition experiment showed that Et_4NCN reacts with $\text{Fe}_2(\text{S}_2\text{C}_3\text{H}_6)(\text{CO})_6$ more rapidly than with $(\text{Et}_4\text{N})[\text{Fe}_2(\text{S}_2\text{C}_3\text{H}_6)(\text{CN})(\text{CO})_5]$. Salts of $[\text{Fe}_2(\text{SR})_2(\text{CN})_2(\text{CO})_4]^{2-}$ (for $(\text{SR})_2 = (\text{SMe})_2$ and $\text{S}_2\text{C}_2\text{H}_4$) and the monocyanides $[\text{Fe}_2(\text{S}_2\text{C}_3\text{H}_6)(\text{CN})(\text{CO})_5]^-$ and $[\text{Fe}_2(\text{S}-t\text{-Bu})_2(\text{CN})(\text{CO})_5]^-$ were characterized crystallographically; in each case, the Fe–CO distances were $\sim 10\%$ shorter than the Fe–CN distances. The oxidation potentials for $\text{Fe}_2(\text{S}_2\text{C}_3\text{H}_6)(\text{CO})_4\text{L}_2$ become milder for $\text{L} = \text{CO}$, followed by MeNC , PMe_3 , and CN^- ; the range is ~ 1.3 V. In water, oxidation of $[\text{Fe}_2(\text{S}_2\text{C}_3\text{H}_6)(\text{CN})_2(\text{CO})_4]^{2-}$ occurs irreversibly at -0.12 V ($\text{Ag}|\text{AgCl}$) and is coupled to a second oxidation.

Introduction

The dinuclear hexacarbonyls of the general formula $\text{Fe}_2(\text{SR})_2(\text{CO})_6$ have been known for over 70 years. Reihlen first prepared $\text{Fe}_2(\text{SEt})_2(\text{CO})_6$ by the carbonylation of aqueous $\text{Fe}(\text{II})$ solutions in the presence of NaSEt via a procedure that was modeled after Pavel's preparation of $\text{Fe}_2(\text{SEt})_2(\text{NO})_4$.¹ Hieber and Spacu prepared $\text{Fe}_2(\text{SR})_2(\text{CO})_6$ via the reaction of thiols and $\text{Fe}(\text{CO})_5$.² In the 1960s, King separated $\text{Fe}_2(\text{SMe})_2(\text{CO})_6$ into three isomers demonstrating the stereochemical features associated with the bridging mercaptide group.³ In the 1980s, Seyferth et al. developed a synthesis of $[\text{Fe}_2(\text{S})_2(\text{CO})_6]^{2-}$, an analogue of Roussin's red anion $[\text{Fe}_2(\text{S})_2(\text{NO})_4]^{2-}$,⁴ and showed that this carbonyl anion could be alkylated to give $\text{Fe}_2(\text{SR})_2(\text{CO})_6$.⁵ In part, because of their considerable stability, many examples of $\text{Fe}_2(\text{SR})_2(\text{CO})_6$ have been reported, and extensive research describes the physical and chemical properties of such compounds.

Until recently, it was generally assumed that the essential chemistry of $\text{Fe}_2(\text{SR})_2(\text{CO})_6$ was mature. It was, therefore, a great surprise when crystallographic investigations of the so-called Fe-only hydrogenases revealed a six-iron "H-cluster" containing an $\text{Fe}_2(\mu\text{-SR})_2(\text{CN})_2(\text{CO})_3\text{L}_n$ core ($\text{L} = \text{H}_2\text{O}$ and a thiolate-linked $\text{Fe}_4\text{S}_4(\text{SR})_4$ cluster).^{6,7} Whereas the diiron core

bears a structural similarity to the Reihlen hexacarbonyls, there are seven ligands and the Fe–Fe bond length of 2.6 Å is ~ 0.1 Å longer than it is in the iron thiolate tricarbonyl dimers.⁸ IR studies also showed that the hydrogenases bind CO, which explains the ability of CO to inhibit the enzyme. The inhibiting CO binds in the position occupied by water in one of the crystallized enzymes; this same site is assumed to be the position for binding H_2 .⁹ The coordination chemistry of the Fe-only hydrogenases is also reminiscent of that of the Fe–Ni hydrogenases, which feature an $\text{Fe}(\text{CN})_2(\text{CO})$ center linked via a pair of thiolato ligands to a nickel center.¹⁰ There is little or no sequence homology between these two families of hydrogenase enzymes; that is, they appear to have evolved independently.¹¹ More recently still, Fontecilla-Camps has proposed that the Fe_2 centers are linked by the azadithiolate $\text{SCH}_2\text{NH}_x\text{CH}_2\text{S}$.⁷ A synthetic analogue supporting this hypothesis has been reported by us.¹²

(6) Peters, J. W.; Lanzilotta, W. N.; Lemon, B. J.; Seefeldt, L. C. *Science* **1998**, 282, 1853–1858. Nicolet, Y.; Piras, C.; Legrand, P.; Hatchikian, C. E.; Fontecilla-Camps, J. C. *Structure* **1999**, 7, 13–23.

(7) Nicolet, Y.; de Lacey, A. L.; Vernède, X.; Fernandez, V. M.; Hatchikian, E. C.; Fontecilla-Camps, J. C. *J. Am. Chem. Soc.* **2001**, 123, 1596–1601.

(8) Dahl, L. F.; Wei, C. H. *Inorg. Chem.* **1963**, 2, 328–333.

(9) Lemon, B. J.; Peters, J. W. *Biochemistry* **1999**, 38, 12969–12973. De Lacey, A. L.; Stadler, C.; Cavazza, C.; Hatchikian, E. C.; Fernandez, V. M. *J. Am. Chem. Soc.* **2000**, 122, 11232–11233.

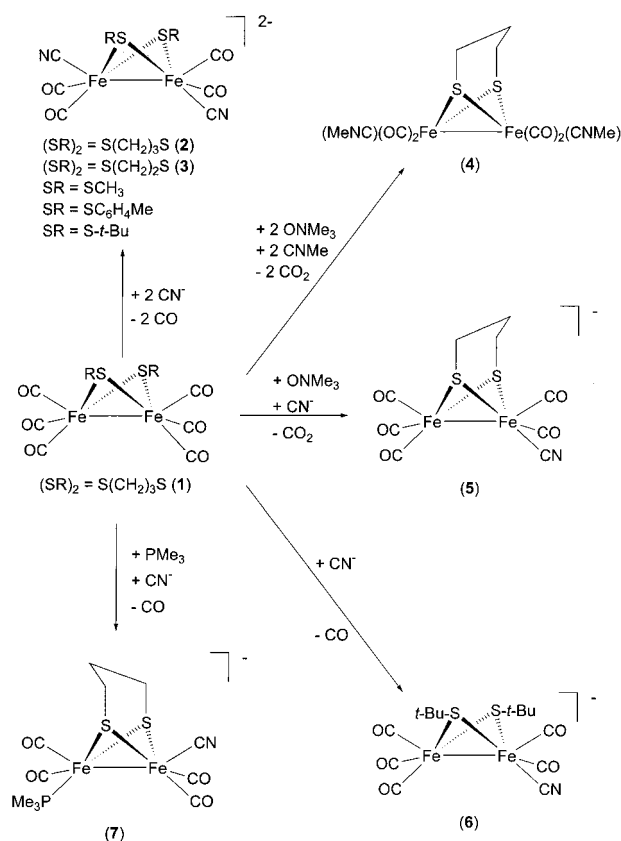
(10) Fontecilla-Camps, J. C.; Ragsdale, S. W. *Adv. Inorg. Chem.* **1999**, 47, 283–333.

(11) Adams, M. W. W.; Stiefel, E. I. *Curr. Opin. Chem. Biol.* **2000**, 4, 214–220.

(12) Lawrence, J. D.; Li, H.; Rauchfuss, T. B.; Rohmer, M.-M.; Bénard, M. *Angew. Chem., Int. Ed. Engl.* **2001**, 40, 1768–1771.

- (1) Pavel, O. *Ber. Dtsch. Chem. Ges.* **1882**, 15, 2600–2615.
 (2) Hieber, W.; Spacu, P. Z. *Anorg. Allgem. Chem.* **1937**, 233, 852–864. Reihlen, H.; Gruhl, A.; Hessling, G. v. *Liebigs Ann. Chem.* **1929**, 472, 268–287.
 (3) King, R. B. *J. Am. Chem. Soc.* **1962**, 84, 2460.
 (4) Roussin, M. L. *Ann. Chim. Phys.* **1858**, 52, 285–303.
 (5) Seyferth, D.; Henderson, R. S.; Song, L. C. *Organometallics* **1982**, 1, 125–133.

Scheme 1

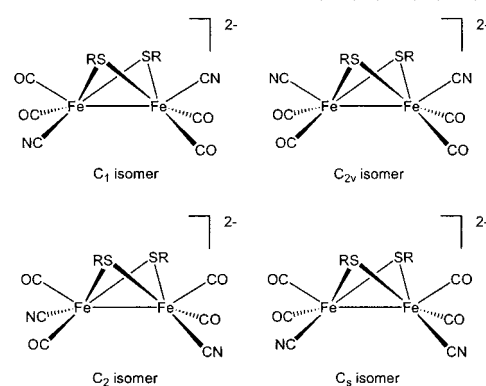


Our previous communication described the synthesis and structural characterization of $(\text{Et}_4\text{N})_2[\text{Fe}_2(\text{S}_2\text{C}_3\text{H}_6)(\text{CN})_2(\text{CO})_4]$.¹³ In the course of that work, a number of questions came to the fore that we address in this report. These questions are, in turn, (i) the effect of diverse dithiolates on the structural chemistry of the dicyanides, (ii) the elusiveness of the monocyanide derivatives, and (iii) the effect of CN^- -for- CO substitution on the redox properties of these dimers. In this work, we examined the products resulting from the reaction of cyanide with the Reihlen dimers. Our intention was to generate a range of dicyano derivatives that could be used in subsequent modeling experiments. In recent work, we indeed show that members of this class of compounds are effective catalysts for hydrogen evolution from protons.¹⁴

Results

Synthesis of $[\text{Fe}_2(\text{SR})_2(\text{CN})_2(\text{CO})_4]^{2-}$. The deep red $[\text{Fe}_2(\text{SR})_2(\text{CN})_2(\text{CO})_4]^{2-}$ derivatives were prepared by treatment of MeCN solutions of $\text{Fe}_2(\text{SR})_2(\text{CO})_6$ with 2 equiv of Et_4NCN . IR and ^1H NMR spectra indicated total consumption of the starting hexacarbonyl in 30–60 min at room temperature. The dicyanides are unreactive toward further equivalents of cyanide (Scheme 1).

IR spectra of the dicyanides feature three bands and a shoulder between 1965 and 1870 cm^{-1} assigned to ν_{CO} ; we also observe bands at 2077 and 2033 cm^{-1} for ν_{CN} . IR spectra of all dicyano species are quite similar, with a variation of no more than a few wavenumbers between derivatives. As originally demonstrated by King many years ago for the SMe derivative,³ the ^1H NMR spectrum of $\text{Fe}_2(\text{SR})_2(\text{CO})_6$ ($\text{R} = \text{alkyl}$) consists of

Chart 1. Geometric Isomers of $[\text{Fe}_2(\text{SR})_2(\text{CN})_2(\text{CO})_4]^{2-}$ 

three signals assigned to the diequatorial (idealized C_{2v}) and axial–equatorial (C_1 symmetry) isomers, henceforth referred to as *e,e* and *a,e* isomers. A similar situation applies to the dicyanides derived from monothiolates. Ignoring the orientation of the alkyl substituent, four geometric isomers of $[\text{Fe}_2(\text{SR})_2(\text{CN})_2(\text{CO})_4]^{2-}$ are possible (Chart 1).

Although differences in the IR spectra of *e,e* and *a,e* isomers could be observed in nonpolar solvents, no indication of isomerism appeared in the ν_{CO} bands of the dicyano species in MeCN. The observed bands are broader because of the increased polarity of the solvent required to dissolve these species; this solvent-induced broadening may mask minor differences in the IR signals of the individual isomers. Both the *a,e* and *e,e* isomers of $(\text{Et}_4\text{N})_2[\text{Fe}_2(\text{SMe})_2(\text{CN})_2(\text{CO})_4]$ cocrystallize, and these contributors were resolved in the refinement.¹⁵ The location of the CN^- ligand differs for the *e,e* and *a,e* isomers, indicative of the small difference in energy between the various cyanide positions. There is no obvious pattern for the variations in the *a,e/e,e* ratio between the hexacarbonyl and the corresponding dicyano compounds (see Experimental Section). It was previously proposed that axially oriented substituents are favored by steric repulsions with the basal CO ligands and that equatorial substituents are favored by bulky donor ligands on the Fe.¹⁶

In addition to the SMe derivative, we also prepared the corresponding thiocresolate derivative $(\text{Et}_4\text{N})_2[\text{Fe}_2(\text{SC}_6\text{H}_4\text{Me})_2(\text{CN})_2(\text{CO})_4]$. Again, the *a,e/e,e* ratio differs for the hexacarbonyl and dicyano compounds. Compound 3 was employed in a test for the involvement of monometallic intermediates in the cyanide substitution reactions. Treatment of excess CN^- with a 1:1 mixture of $\text{Fe}_2(\text{SMe})_2(\text{CO})_6$ and $\text{Fe}_2(\text{SC}_6\text{H}_4\text{Me})_2(\text{CO})_6$ gave only $(\text{Et}_4\text{N})_2[\text{Fe}_2(\text{SMe})_2(\text{CN})_2(\text{CO})_4]$ and $(\text{Et}_4\text{N})_2[\text{Fe}_2(\text{SC}_6\text{H}_4\text{Me})_2(\text{CN})_2(\text{CO})_4]$. No ^1H NMR signals were observed that could be assigned to the mixed thiolato derivatives.

Because structural studies on the H-cluster indicate a chelating dithiolate ligand, we examined the cyanide substitution of a variety of chelating dithiolato derivatives $\text{Fe}_2(\mu\text{-SXS})(\text{CO})_6$ ($\text{X} = \text{CR}_2, \text{C}_2\text{H}_4, \text{C}_3\text{H}_6$). We were unable to prepare cyanide-substituted derivatives of 1,1-dithiolates, $\text{Fe}_2(\text{S}_2\text{CR}_2)(\text{CO})_6$, including methanedithiolate¹⁷ and 2,2-adamantanedithiolate.¹⁸ These hexacarbonyl derivatives react with Et_4NCN , but NMR analysis suggests that side reactions occur at the organosulfur ligands, possibly involving C–S bond cleavage. Furthermore,

(13) Schmidt, M.; Contakes, S. M.; Rauchfuss, T. B. *J. Am. Chem. Soc.* **1999**, *121*, 9736–9737.

(14) Gloaguen, F.; Lawrence, J. D.; Rauchfuss, T. B. *J. Am. Chem. Soc.* **2001**, *123*, 9476–9477.

(15) Contakes, S. M. *Synthesis of Novel Organometallic Cyanometalates and Phthalocyanines*. Ph.D. Dissertation, University of Illinois, Urbana, IL, 2001.

(16) Maresca, L.; Greggio, F.; Sbrignadello, G.; Bor, G. *Inorg. Chim. Acta* **1971**, *5*, 667–674.

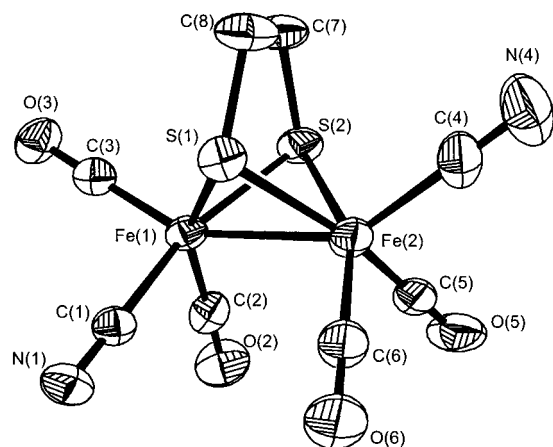


Figure 1. Structure of the dianion in $(\text{Et}_4\text{N})_2[\text{Fe}_2(\text{S}_2\text{C}_2\text{H}_4)(\text{CN})_2(\text{CO})_4]$ (**3**) with the thermal ellipsoids set at the 50% probability level. Selected distances (Å) and angles (deg): Fe(1)–Fe(2), 2.5114(12); Fe(1)–C(1), 1.924(6); Fe(1)–C(2), 1.759(7); Fe(1)–C(3), 1.762(6); Fe(2)–C(4), 1.944(7); Fe(2)–C(5), 1.716(7); Fe(2)–C(6), 1.753(6); Fe(1)–S(1), 2.2446(17); Fe(1)–S(2), 2.2451(17); Fe(2)–S(1), 2.2737(18); Fe(2)–S(2), 2.2652(16); S(1)–Fe(1)–S(2), 80.68(6); S(1)–Fe(2)–S(2), 79.63(6).

the benzenedithiolate $\text{Fe}_2(\text{S}_2\text{C}_6\text{H}_4)(\text{CO})_6$ was found to react with Et_4NCN resulting in redox reactions; these results are reported separately.¹⁹

The solid-state structure of the 1,2-ethanedithiolate $(\text{Et}_4\text{N})_2[\text{Fe}_2(\text{S}_2\text{C}_2\text{H}_4)(\text{CN})_2(\text{CO})_4]$ (CN = ^{12}CN , **3**, CN = ^{13}CN , **3a**) is nearly identical to that of the previously reported propanedithiolate derivative,¹³ with the CN ligands positioned for the C_1 isomer (Figure 1). The most significant difference between the two chelating dithiolato derivatives is the contraction of the S–Fe–S angles by approximately 5° in the 1,2-ethanedithiolate. This S–Fe–S angle contracts by an additional 8° in 1,1-dithiolate $\text{Fe}_2[\text{S}_2\text{CHCH}_2\text{C}(\text{O})\text{CH}_3](\text{CO})_6$.²⁰

The dynamic properties of the new complexes were checked by variable temperature NMR spectroscopy. It was already known that species of the type $\text{Fe}_2(\text{SR})_2(\text{CO})_6$ exist as isomers on the basis of the relative orientation of the R groups, which can be axial or equatorial, and Huttner had demonstrated that the backbone of chelating dithiolate derivatives, for example, $\text{Fe}_2(\text{S}_2\text{C}_n\text{H}_{2n})(\text{CO})_6$, undergo ring refolding on the NMR time scale.²¹ $\text{Fe}_2(\text{S}_2\text{C}_3\text{H}_6)(\text{CO})_6$ (**1**) shows a single CO resonance at 25°C that splits into two singlets with intensity 2:1 at -80°C , consistent with the solid-state structure. In the room temperature ^{13}C NMR spectrum of the dicyano derivatives, the CO and CN^- ligands appear as singlets because of a low-energy turnstile interchange of the CO and CN^- sites. The ^{13}C NMR spectrum of ^{13}CN -enriched (30%) $[\text{Fe}_2(\text{S}_2\text{C}_2\text{H}_4)(\text{CN})_2(\text{CO})_4]^{2-}$ in the CN region consisted of four singlets at -80°C with rough integrations of 1:3:3:2. On the basis of the number of isomers for the $[\text{Fe}_2(\text{SR})_2(\text{CN})_2(\text{CO})_4]^{2-}$ core, a maximum of five CN signals are expected. A similar pattern is seen in the ^{13}C NMR spectrum of **2a**, that is, four CN signals at low temperatures. In

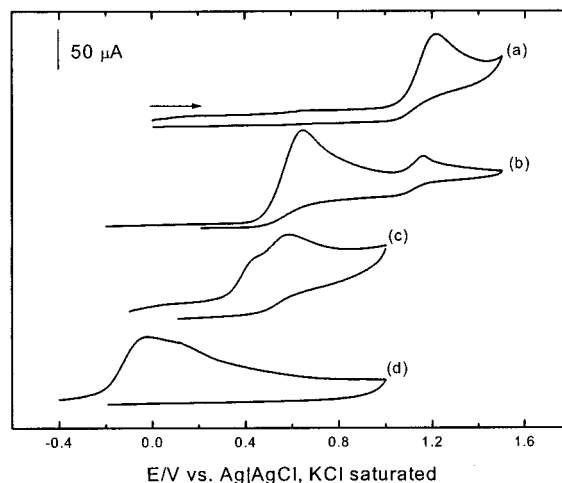


Figure 2. Voltammograms (200 mV s^{-1}) of $\text{Fe}_2(\text{S}_2\text{C}_3\text{H}_6)(\text{CO})_6$ (**a**), $\text{Fe}_2(\text{S}_2\text{C}_3\text{H}_6)(\text{CNMe})_2(\text{CO})_4$ (**b**), $(\text{Et}_4\text{N})[\text{Fe}_2(\text{S}_2\text{C}_3\text{H}_6)(\text{CN})(\text{CO})_5]$ (**c**), and $(\text{Et}_4\text{N})_2[\text{Fe}_2(\text{S}_2\text{C}_3\text{H}_6)(\text{CN})_2(\text{CO})_4]$ (**d**) in $\text{MeCN}-\text{Bu}_4\text{NPF}_6$ at a glassy carbon electrode. Anodic currents are positive.

Table 1. Redox Potentials of $\text{Fe}_2(\text{S}_2\text{C}_3\text{H}_6)(\text{CO})_6\text{-L}_x$ (L = CO, PMe_3 , CNMe, CN^-). Potentials Are Quoted against the $\text{Ag}|\text{AgCl}$ Reference Electrode ($\sim -0.2\text{ V}$ vs NHE)

compound	E^{red1}/V	E^{ox1}/V
$\text{Fe}_2(\text{S}_2\text{C}_3\text{H}_6)(\text{CO})_6^a$	-1.25^c	
$\text{Fe}_2(\text{S}_2\text{C}_3\text{H}_6)(\text{CO})_6^b$	-1.16^c	1.2^d
$\text{Fe}_2(\text{S}_2\text{C}_3\text{H}_6)(\text{CO})_5(\text{CNMe})^b$	-1.37^d	1.01^d
$\text{Fe}_2(\text{S}_2\text{C}_3\text{H}_6)(\text{CO})_4(\text{CNMe})_2^b$	-1.64^d	0.65^d
$[\text{Fe}_2(\text{S}_2\text{C}_3\text{H}_6)(\text{CN})(\text{CO})_5]^{-b}$	-1.73^d	0.57^d
$\text{Fe}_2(\text{S}_2\text{C}_3\text{H}_6)(\text{CO})_4(\text{PMe}_3)^b$	-1.86^d	0.24^c
$[\text{Fe}_2(\text{S}_2\text{C}_3\text{H}_6)(\text{CN})(\text{CO})_4(\text{PMe}_3)]^{-b}$	-2.14^d	0.05^d
$[\text{Fe}_2(\text{S}_2\text{C}_3\text{H}_6)(\text{CN})_2(\text{CO})_4]^{2-b}$	-2.28^d	$-0.08, 0.10^d$

^a THF– Bu_4NPF_6 . ^b MeCN– Bu_4NPF_6 . ^c Reversible. ^d Irreversible.

the case of **2a**, we conclude that the orientation of the trimethylene group has no effect on the ^{13}C NMR shifts of the CN signals.

Redox Properties. Because the hydrogenase enzymes exist in at least two oxidation states,²² we were interested in probing the redox properties of the dicyano species as well as related derivatives. To facilitate comparisons, we focused especially on the 1,3-propanedithiolate derivatives (Figure 2, Table 1).

Cyclic voltammetry (CV) measurements indicate that the first reduction of $\text{Fe}_2(\text{S}_2\text{C}_3\text{H}_6)(\text{CO})_6\text{-L}_x$ ($x = 1, 2$; L = CNMe, PMe_3 , CN^-) is irreversible, whereas the first reduction of the hexacarbonyl complex is reversible. Hexacarbonyl **1** undergoes irreversible oxidation at $E_p = 1.21\text{ V}$. This oxidation reaction involves two electrons on the basis of a comparison of i_p values versus the first reduction ($E_{1/2}^{\text{red1}} = -1.16\text{ V}$). Oxidation of **1** generates a species that undergoes irreversible reduction at -0.98 V , as detected on the reverse scan. In other words, oxidation of **1** follows an EC_i mechanism whereby the oxidation product is reducible at -0.98 V . Upon controlled-potential electrolysis, oxidation of **1** at 1.21 V requires $\sim 1.8\text{ F mol}^{-1}$. The voltammogram recorded after electrolysis does not show the -0.98 V reduction peak, indicative of the instability of the oxidized species. Indeed, the IR spectrum of the electrolyzed solution shows no ν_{CO} bands. The species generated by reduction of a solution of **1** were found to be also unstable on the time scale of electrolysis.

Study of the redox properties of $(\text{Et}_4\text{N})_2[\text{Fe}_2(\text{S}_2\text{C}_3\text{H}_6)(\text{CN})_2(\text{CO})_4]$ (**2**) at anodic potential was difficult because a passivating

(17) Seyferth, D.; Womack, G. B.; Gallagher, M. K.; Cowie, M.; Hames, B. W.; Fackler, J. P., Jr.; Mazany, A. M. *Organometallics* **1987**, *6*, 283–294.

(18) Alper, H.; Chan, A. S. K. *Inorg. Chem.* **1974**, *13*, 232–236. We confirmed the structure of $\text{Fe}_2(\text{S}_2\text{-2,2-C}_{10}\text{H}_{14})(\text{CO})_6$: Linck, R. C. Unpublished results.

(19) Rauchfuss, T. B.; Contakes, S. M.; Hsu, S. C. N.; Reynolds, M. A.; Wilson, S. R. *J. Am. Chem. Soc.* **2001**, *123*, 6933–6934.

(20) Seyferth, D.; Womack, G. B.; Song, L. C.; Cowie, M.; Hames, B. W. *Organometallics* **1983**, *2*, 928–930.

(21) Winter, A.; Zsolnai, L.; Huttner, G. Z. *Naturforsch.* **1982**, *37b*, 1430–1436.

(22) Pierik, A. J.; Hulstein, M.; Hagen, W. R.; Albracht, S. P. J. *Eur. J. Biochem.* **1998**, *258*, 572–578.

blue film is deposited on the electrode surface at $E > 1.0$ V, necessitating polishing of the electrode between experiments. Electropolymerization of **1** upon oxidation was confirmed by controlled-potential electrolysis. The primary oxidation occurs at $E_p^{ox1} = -0.08$ (the oxidation peak shows a shoulder at 0.10 V), and the primary reduction occurs at $E_p^{red1} = -2.28$ V. The observed peak potential value agrees with that previously reported by Le Cloirec et al.²³ The first oxidation of **2** is assigned to a one-electron process in comparison of the peak current with that of $\{Ni[S_2C_2(CN)_2]_2\}^{2-}$, an internal standard whose diffusion coefficient is expected to be comparable to that of **2**. As previously reported,²³ **2** is both soluble and stable in aqueous electrolyte. No deposition of insoluble species was observed upon oxidation of **2** in aqueous media, suggesting that the oxidation product is different from that generated in MeCN. At pH = 5 (phthalate buffer), the first (irreversible) oxidation occurs at -0.12 V ($\sim +0.38$ V vs RHE), indicating that **2** cannot directly reduce protons in aqueous electrolyte at this pH. No catalytic behavior of **2** toward proton reduction was observed.

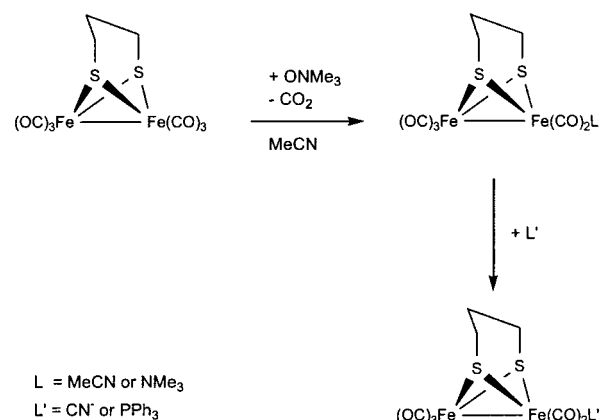
Oxidation of THF solutions of bis(isocyanide) **4** appears to produce insoluble species causing passivation of the electrode. In MeCN solution, however, the CV of **4** shows an oxidation peak (0.65 V), less anodic than for the parent complex **1**, consistent with the superior donor properties of CNMe versus CO ligands.²⁴ Similar redox behavior was reported by Poilblanc et al.,²⁵ for $Fe_2(SMe)_2(CO)_4(PMe_3)_2$.

Oxidation of $(Et_4N)[Fe_2(S_2C_3H_6)(CN)(CO)_5]$ (**5**) did not produce any insoluble species blocking the electrode surface, in contrast to the behavior of **2**. The first oxidation of **5** occurs at $E_p^{ox1} = 0.57$ V, and the first reduction at $E_p^{red1} = -1.73$ V, indicating that, as expected, **5** is more difficult to oxidize and easier to reduce than dicyanide **2** (see above). The ratio $i_{p^{ox1}}/i_{p^{red1}}$ is ~ 0.5 , suggesting that the oxidation and the reduction of **5** are one- and two-electron processes, respectively.

Poilblanc et al. have shown that the complexes of general formula $Fe_2(SR)_2(CO)_4L_2$ are more difficult to reduce and easier to oxidize when CO is replaced by donor ligands such as tertiary phosphines.²⁵ In the present work, we found that the reduction becomes more cathodic, and the oxidation less anodic in the following sequence: **1** > $Fe_2(S_2C_3H_6)(CO)_5(CNMe)$ > **4** > **5** > $Fe_2(S_2C_3H_6)(CO)_4(PMe_3)_2$ > **2**. With respect to hexacarbonyl **1**, the oxidation and reduction of **2** occur at potentials that are ~ 1.3 V less positive and 1.2 V more negative, respectively. This suggests that, beyond a possible role in hydrogen-bonding, the cyanide and phosphine ligands modify the redox properties of **1** in a similar way, that is, by acting as a strong donor ligand. According to Le Cloirec et al.,²³ the hydrogenase active site ("H-cluster") would be easier to oxidize than **2** to drive proton reduction. Direct redox is, however, not the only mechanism to consider. Another possibility involves a chemical reaction between the bimetallic subunit and the protons to form a metal hydride complex, which upon subsequent reduction could produce hydrogen. Indeed, other complexes of the type $Fe_2-(SR)_2(CO)_4(PMe_3)_2$, which exhibit similar redox properties to those of **2**, are well-known to protonate at the Fe–Fe bond.^{25b}

Synthesis of the Monocyano Derivatives of $Fe_2(S_2C_3H_6)(CO)_6$. In this part of the study, we explored the preparation of monosubstituted derivatives of the type $[Fe_2(S_2C_3H_6)(CN)(CO)_5]^-$.

Scheme 2



These experiments were motivated by the instability reported²⁶ for $Na[Fe_2(S_2C_3H_6)(CN)(CO)_5]$. We first developed routes to the desired monocyano salts using the decarbonylation agent Me_3NO (Scheme 2). Initial experiments confirmed that solutions of **1** and PPh_3 react at room temperature only upon addition of Me_3NO . The product, $Fe_2(S_2C_3H_6)(CO)_5(PPh_3)$, was identified by its characteristic IR spectrum.²⁷ We found that the PPh_3 could be added well after the decarbonylation agent; this experiment implies that the intermediate, possibly $Fe_2(S_2C_3H_6)(CO)_5-(MeCN)$ or $Fe_2(S_2C_3H_6)(CO)_5(NMe_3)$, has significant lifetime in solution (Scheme 2). In fact, the IR spectrum of such solutions demonstrated the absence of **1** and the formation of a pattern typical of $Fe_2(S_2C_3H_6)(CO)_5L$. Attempts to isolate this complex were unsuccessful.

Salts of $[Fe_2(S_2C_3H_6)(CN)(CO)_5]^-$ had been previously obtained via the reaction of $NaN(tms)_2$ with $Fe_2(S_2C_3H_6)(CO)_6$,^{26,28} a method that obviates the use of free CN^- . The Na^+ salt is apparently unstable, even in the solid state under an inert atmosphere.²⁶ The corresponding Et_4N^+ salt was, however, completely stable even in solution for days. Analytically pure samples of $(Et_4N)[Fe_2(S_2C_3H_6)(CN)(CO)_5]$ (**5**) were obtained via the reaction of $Fe_2(S_2C_3H_6)(CO)_6$ with Me_3NO followed by addition of Et_4NCN (Scheme 2). The structure of **5** was confirmed by single-crystal X-ray diffraction (Figure 3). The 1H NMR spectrum of this monocyano in the $(CH_2)_3$ region consists of two broad signals at room temperature that split into four multiplets at -40 °C. The overall pattern is consistent with four types of methylene protons. The room temperature NMR data differ slightly from those described previously in terms of the coupling pattern,²⁶ but this difference may be due to ion pairing effects because alkali metal cations are well-known to bind to MCN (e.g., $Na_2Fe(CN)_4(CO)_2(dmf)_4$).²⁹ In the IR spectrum of **5**, all ν_{CO} bands are shifted toward lower energies (vs **1**) indicating that the cyanide influences *both* Fe centers strongly. Similar electronic effects have been previously noted for the phosphine derivatives.^{16,30}

Having established the considerable stability of **5**, we were perplexed by our inability to directly synthesize this species from the reaction of 1 equiv of CN^- and $Fe_2(S_2C_3H_6)(CO)_6$. For example, the activation parameters reported²⁶ for the reaction of Et_4NCN with hexacarbonyl **1** and with **5** suggested that it should be possible to generate at least some of the monocyanoide

(23) Le Cloirec, A.; Best, S. P.; Borg, S.; Davies, S. C.; Evans, D. J.; Hughes, D. L.; Pickett, C. J. *Chem. Commun.* **1999**, 2285–2286.

(24) Madec, P.; Muir, K. W.; Pétillon, F. Y.; Rumin, R.; Scaon, Y.; Schollhammer, P.; Talarmin, J. J. *Chem. Soc., Dalton Trans.* **1999**, 2371–2383.

(25) (a) Mathieu, R.; Poilblanc, R.; Lemoine, P.; Gross, M. J. *Organomet. Chem.* **1979**, 165, 243–252. (b) Arabi, M. S.; Mathieu, R.; Poilblanc, R. J. *Organomet. Chem.* **1979**, 177, 199–209.

(26) Lyon, E. J.; Georgakaki, I. P.; Reibenspies, J. H.; Darensbourg, M. Y. *J. Am. Chem. Soc.* **2001**, 123, 3268–3278.

(27) Ellgen, P. C.; Gerlach, J. N. *Inorg. Chem.* **1973**, 12, 2526–2532.

(28) Lyon, E. J.; Georgakaki, I. P.; Reibenspies, J. H.; Darensbourg, M. Y. *Angew. Chem., Int. Ed. Engl.* **1999**, 38, 3178–3180.

(29) Jiang, J.; Koch, S. A. *Angew. Chem., Int. Ed. Engl.* **2001**, 40, 2629–2631.

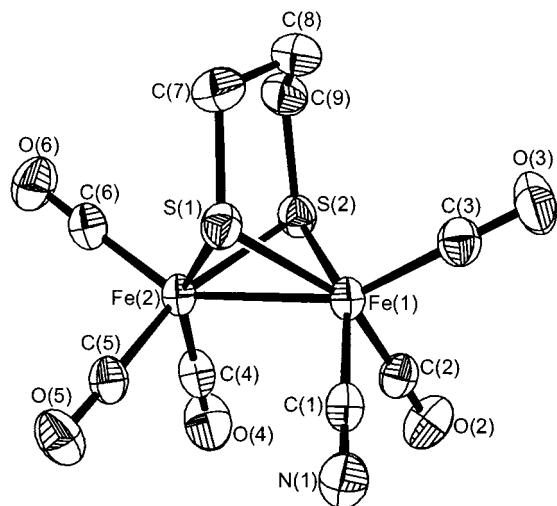
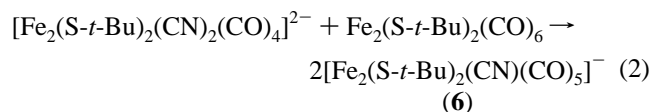
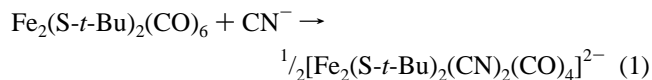


Figure 3. Structure of the anion in $(\text{Et}_4\text{N})[\text{Fe}_2(\text{S}_2\text{C}_3\text{H}_6)(\text{CN})(\text{CO})_5]$ (**5**) with the thermal ellipsoids set at the 50% probability level. Selected distances (Å) and angles (deg): Fe(1)–Fe(2), 2.5291(6); Fe(1)–C(1), 1.923(3); Fe(1)–C(2), 1.771(3); Fe(1)–C(3), 1.773(3); Fe(2)–C(4), 1.768(3); Fe(2)–C(5), 1.791(3); Fe(2)–C(6), 1.797(3); Fe(1)–S(1), 2.2520(8); Fe(1)–S(2), 2.2518(8); Fe(2)–S(1), 2.2678(8); Fe(2)–S(2), 2.2698(8); S(1)–Fe(1)–S(2), 85.80(3); S(1)–Fe(2)–S(2), 85.01(3).

from the room-temperature reaction of **1** and Et_4NCN . Careful study revealed that $\sim 15\%$ yields of **5** can be realized by direct reaction with 1 equiv of Et_4NCN in both concentrated and dilute MeCN solutions of **1** (0.1–0.01 M).

Synthesis of the Monocyno Derivatives of $\text{Fe}_2(\text{S-}t\text{-Bu})(\text{CO})_6$. Treatment of $\text{Fe}_2(\text{S-}t\text{-Bu})_2(\text{CO})_6$ with an excess of cyanide led exclusively to the dicyano species, which was identified by its characteristic IR spectrum in the ν_{CO} region.^{13,23,28} Furthermore, the ^1H NMR spectrum of the dicyanide consists of three signals for the *t*-Bu group in a ratio of 1:1:0.28 indicative of both *e,e* and *a,e* isomers as seen for $\text{Fe}_2(\text{S-}t\text{-Bu})_2(\text{CO})_6$.³¹ Solutions of $[\text{Fe}_2(\text{S-}t\text{-Bu})_2(\text{CN})_2(\text{CO})_4]^{2-}$ are, however, unstable, decomposing over a period of days leaving free *t*-BuSH as the only identifiable product. The reaction of $\text{Fe}_2(\text{S-}t\text{-Bu})_2(\text{CO})_6$ with 1 equiv of Ph_4PCN affords two new products, the monocyno ($\text{Ph}_4\text{P})[\text{Fe}_2(\text{S-}t\text{-Bu})_2(\text{CN})(\text{CO})_5]$ (**6b**) (see later) and the dicyanide (Figure 4). Over 2 days in solution, the signals due to the dicyanide and unreacted hexacarbonyl decrease in intensity concomitant with the increase in intensity of the signals for the monocyanide. Some free *t*-BuSH is also observed. These observations led us to speculate that the monocyanide arises via decomposition of $[\text{Fe}_2(\text{S-}t\text{-Bu})_2(\text{CN})_2(\text{CO})_4]^{2-}$ in the presence of $\text{Fe}_2(\text{S-}t\text{-Bu})_2(\text{CO})_6$, which serves as a trapping agent for cyanide (eqs 1, 2).



The PPh_4^+ salt of $[\text{Fe}_2(\text{S-}t\text{-Bu})_2(\text{CN})(\text{CO})_5]^-$ was isolated in nearly analytical purity and was further characterized by IR and

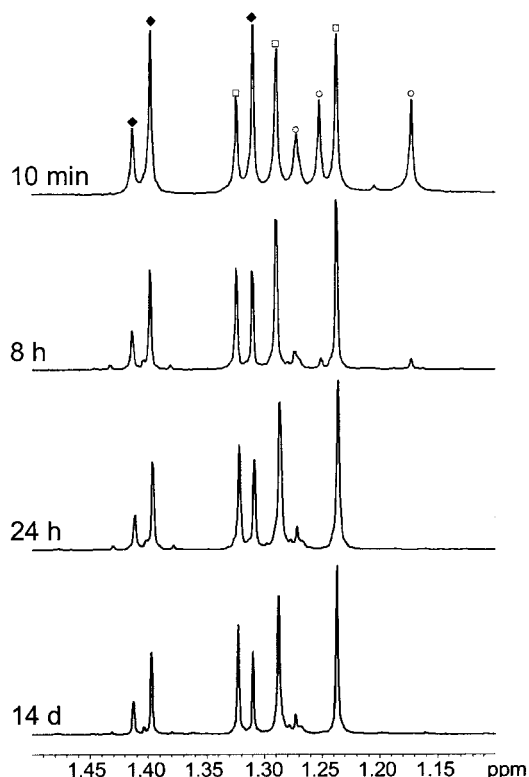


Figure 4. 500 MHz NMR spectra of the reaction of $\text{Fe}_2(\text{S-}t\text{-Bu})_2(\text{CO})_6$ with 1 equiv of Et_4NCN in CD_3CN . Open circles (○) correspond to $\text{Fe}_2(\text{S-}t\text{-Bu})_2(\text{CO})_6$, open squares (□) correspond to $[\text{Fe}_2(\text{S-}t\text{-Bu})_2(\text{CN})_2(\text{CO})_4]^{2-}$ (**6**), and filled diamonds (◆) correspond to $[\text{Fe}_2(\text{S-}t\text{-Bu})_2(\text{CN})(\text{CO})_5]^-$ (**6b**).

NMR spectroscopy. The IR spectrum of **6b** consists of four bands, one in the CN region and three in the CO region at 2086 cm^{-1} and at 2023, 1969, 1939 cm^{-1} , respectively. Crystals of $\text{K}(18\text{-crown-6})[\text{Fe}_2(\text{S-}t\text{-Bu})_2(\text{CN})(\text{CO})_5]$ (**6c**) were also obtained, and these were examined by single-crystal X-ray diffraction (Figure 5). The solid-state IR spectra of salts **6b** and **6c** in the ν_{CN} ($\text{X} = \text{N}, \text{O}$) region are similar. In the crystal, the anion exists as two enantiomeric units with 89/11% occupancy, situated such that the N of the cyanides are at approximately the same position in the crystal and the Fe–Fe bonds are almost parallel. Otherwise, the structure features the expected five CO ligands indicated by short Fe–CO distances (1.75 Å) and longer Fe–C(N) distances (1.92 Å). The CN group is cis to the Fe–Fe bond in both isomers. The CN terminus is coordinated to K^+ ($r_{\text{N-K}} = 2.70$ Å),³² which is otherwise bound to the six oxygen atoms of the crown ether.

Synthesis of $[\text{Fe}_2(\text{S}_2\text{C}_3\text{H}_6)(\text{CN})(\text{CO})_4(\text{PR}_3)]^-$: Further Insights into the Substitution Mechanism. The logical suggestion^{26,28} that $[\text{Fe}_2(\text{S}_2\text{C}_3\text{H}_6)(\text{CN})(\text{CO})_5]^-$ is an intermediate in the formation of $[\text{Fe}_2(\text{S}_2\text{C}_3\text{H}_6)(\text{CN})_2(\text{CO})_4]^{2-}$ from the hexacarbonyl accords with the finding that isolated samples of $[\text{Fe}_2(\text{S}_2\text{C}_3\text{H}_6)(\text{CN})(\text{CO})_5]^-$ react with Et_4NCN to give $[\text{Fe}_2(\text{S}_2\text{C}_3\text{H}_6)(\text{CN})_2(\text{CO})_4]^{2-}$. This result is necessary but not sufficient evidence for the intermediacy of the pentacarbonyl monocyanide. Further evidence, presented below, points to an alternative pathway for the substitution process; the new evidence was obtained through trapping studies.

When $\text{Fe}_2(\text{S}_2\text{C}_3\text{H}_6)(\text{CO})_6$ is treated with Et_4NCN in the presence of a 4-fold excess of PMe_3 , we obtained $\sim 90\%$ yield of analytically pure $(\text{Et}_4\text{N})[\text{Fe}_2(\text{S}_2\text{C}_3\text{H}_6)(\text{CN})(\text{CO})_4(\text{PMe}_3)]^-$ (**7**).

(30) de Beer, J. A.; Haines, R. J.; Greatrex, R.; Greenwood, N. N. *J. Chem. Soc. A* **1971**, 21, 3271–3282. de Beer, J. A.; Haines, R. J. *J. Organomet. Chem.* **1972**, 37, 173–188. de Beer, J. A.; Haines, R. J. *J. Organomet. Chem.* **1972**, 36, 297–313. de Beer, J. A.; Haines, R. J.; Greatrex, R.; Greenwood, N. N. *J. Organomet. Chem.* **1971**, 27, C33–C35.

(31) Natile, G.; Maresca, L.; Bor, G. *Inorg. Chem. Acta* **1977**, 23, 37–42.

(32) Neier, R.; Trojanowski, C.; Mattes, R. *J. Chem. Soc., Dalton Trans.* **1995**, 2521–2528.

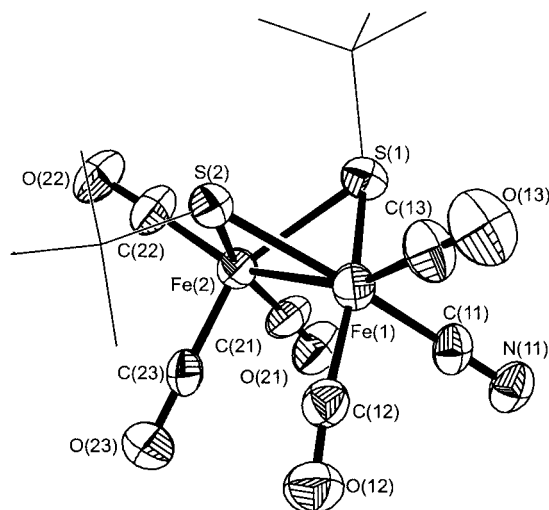


Figure 5. Structure of the major enantiomer of the anion in $[\text{K}(18\text{-crown-6})][\text{Fe}_2(\text{S-}i\text{-Bu})_2(\text{CN})(\text{CO})_5]$ (**6c**) with the thermal ellipsoids set at the 50% probability level. Selected distances (Å) and angles (deg): Fe(1)–Fe(2), 2.506(2); Fe(1)–C(11), 1.912(6); Fe(1)–C(12), 1.736(7); Fe(1)–C(13), 1.735(7); Fe(2)–C(21), 1.730(6); Fe(2)–C(22), 1.777(6); Fe(2)–C(23), 1.728(7); Fe(1)–S(1), 2.290(2); Fe(1)–S(2), 2.251(2); Fe(2)–S(1), 2.285(2); Fe(2)–S(2), 2.264(2); S(1)–Fe(1)–S(2), 79.18(7); S(1)–Fe(2)–S(2), 79.03(8).

This new compound was fully characterized spectroscopically as well as by single crystal X-ray diffraction (Figure 6). Two independent diiron units are found in the unit cell. One of the anions is structurally similar to $\{\text{Fe}_2[\text{S}_2(\text{CH}_2)_n](\text{CN})_2(\text{CO})_4\}^{2-}$ where the basal CN^- has been replaced by PMe_3 .³³ In the other anion in the asymmetric unit, both cyanide and phosphine ligands are basal, being cis to the Fe–Fe bond and trans to the same sulfur atom.

The mechanistic significance of the synthesis of $[\text{Fe}_2(\text{S}_2\text{C}_3\text{H}_6)(\text{CN})(\text{CO})_4(\text{PMe}_3)]^-$ is clarified by the associated control experiments (Scheme 3):

(i) Purified samples of $[\text{Fe}_2(\text{S}_2\text{C}_3\text{H}_6)(\text{CN})(\text{CO})_5]^-$ and PMe_3 react only sluggishly; for example, $[\text{Fe}_2(\text{S}_2\text{C}_3\text{H}_6)(\text{CN})(\text{CO})_4(\text{PMe}_3)]^-$ is formed in low yield (<5%) after 4 h at room temperature, whereas our synthesis of **5** was conducted at -40°C .

(ii) Solutions of $\text{Fe}_2(\text{S}_2\text{C}_3\text{H}_6)(\text{CO})_6$ do not react with excess PMe_3 in 30 min at -10°C . In contrast, the reaction of $\text{Fe}_2(\text{S}_2\text{C}_3\text{H}_6)(\text{CO})_6$ with $\text{Et}_4\text{NCN}/\text{PMe}_3$ is complete after 30 min at -10°C .

Collectively, our observations show that $\text{Fe}_2(\text{S}_2\text{C}_3\text{H}_6)(\text{CO})_6$ reacts with CN^- to produce an intermediate that is more reactive toward PMe_3 than is $[\text{Fe}_2(\text{S}_2\text{C}_3\text{H}_6)(\text{CN})(\text{CO})_5]^-$. Qualitatively similar results were obtained when PPh_3 was employed in place of PMe_3 .

Further evidence that **5** is not an intermediate in the formation of dicyano species **2** from **1** was obtained through a second competition experiment. As a preliminary control, we first showed that a mixture of hexacarbonyl **1** and monocyanide **5** is stable in MeCN solution (Figure 7, spectrum d). Upon treatment of this solution with 2 equiv of Et_4NCN , **1** completely disappeared, but monocyanide **5** remained. The changes are most readily indicated by the disappearance of the ν_{CO} band at $\sim 2000\text{ cm}^{-1}$ and the persistence of the ν_{CN} band at approximately $\sim 2100\text{ cm}^{-1}$ for the monocyanide **5**. Obviously, the monocyano

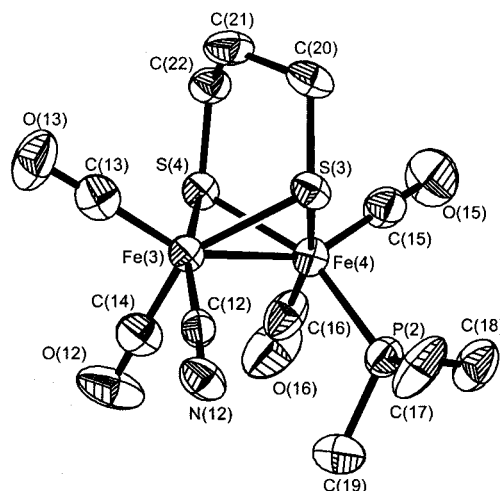
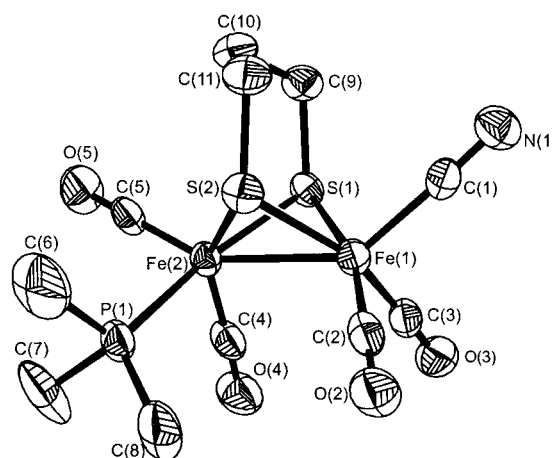
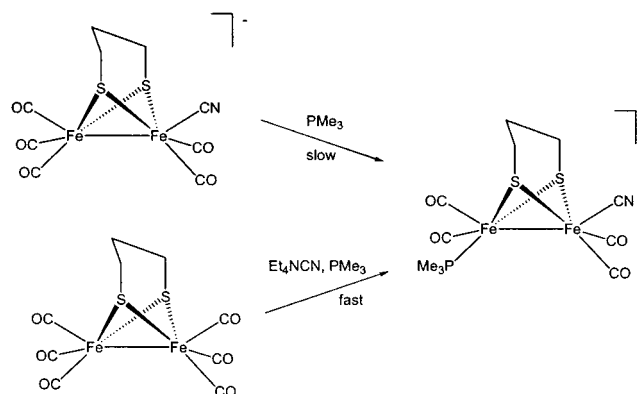


Figure 6. Structure of the anions in $(\text{Et}_4\text{N})[\text{Fe}_2(\text{S}_2\text{C}_3\text{H}_6)(\text{CN})(\text{CO})_4(\text{PMe}_3)]$ (**7**) with the thermal ellipsoids set at the 50% probability level. Selected distances (Å) and angles (deg): (Top) Fe(1)–Fe(2), 2.5365(11); Fe(1)–C(1), 1.919(6); Fe(1)–C(2), 1.742(6); Fe(1)–C(3), 1.741(6); Fe(2)–P(1), 2.2061(16); Fe(2)–C(4), 1.734(6); Fe(2)–C(5), 1.742(6); Fe(1)–S(1), 2.2708(15); Fe(1)–S(2), 2.2629(15); Fe(2)–S(1), 2.2740(15); Fe(2)–S(2), 2.2561(15); S(1)–Fe(1)–S(2), 85.25(5); S(1)–Fe(2)–S(2), 85.33(5). (Bottom) Fe(3)–Fe(4), 2.5593(11); Fe(3)–C(12), 1.920(6); Fe(3)–C(13), 1.766(6); Fe(3)–C(14), 1.747(6); Fe(4)–P(2), 2.2055(17); Fe(4)–C(15), 1.763(6); Fe(4)–C(16), 1.747(7); Fe(3)–S(3), 2.2727(15); Fe(3)–S(4), 2.2560(15); Fe(4)–S(3), 2.2635(15); Fe(4)–S(4), 2.2538(16); S(3)–Fe(3)–S(4), 84.67(5); S(3)–Fe(4)–S(4), 84.93(5).

Scheme 3



species **5** reacts much more slowly with free cyanide than does the hexacarbonyl species **1**.

(33) In contrast, $\text{Fe}_2(\text{SMe})_2(\text{CO})_4(\text{PMe}_3)_2$ and $\text{Fe}_2(\text{SCH}_2\text{CH}_2\text{OH})_2(\text{CO})_4(\text{PPh}_3)_2$ have both phosphines trans to the Fe–Fe bond in the solid state: (a) Le Borgne, G.; Grandjean, D.; Mathieu, R.; Poilblanc, R. *J. Organomet. Chem.* **1977**, *131*, 429–438. (b) Song, L.; Wang, R.; Hu, Q.; Wang, H. *Jiegou Huaxue* **1990**, *9*, 217–220.

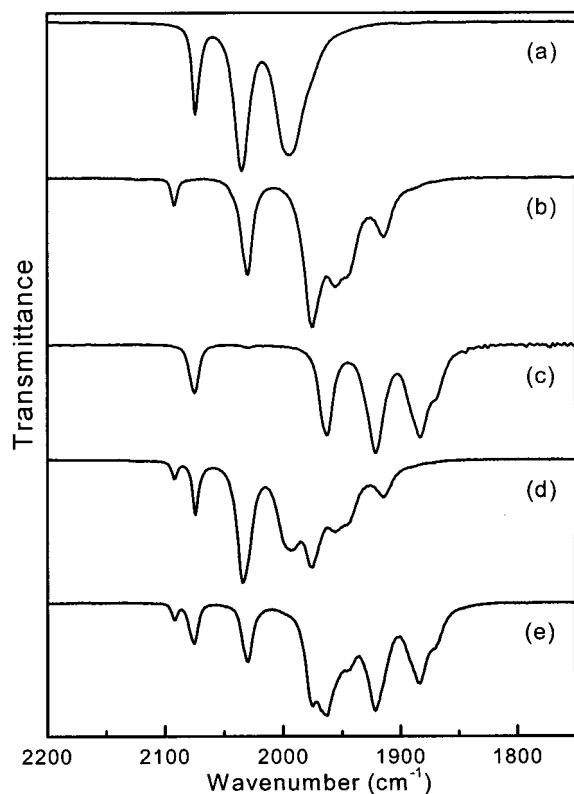


Figure 7. IR spectra (MeCN solution): (a) $\text{Fe}_2(\text{S}_2\text{C}_3\text{H}_6)(\text{CO})_6$, (b) $(\text{Et}_4\text{N})[\text{Fe}_2(\text{S}_2\text{C}_3\text{H}_6)(\text{CN})(\text{CO})_5]$, (c) $(\text{Et}_4\text{N})_2[\text{Fe}_2(\text{S}_2\text{C}_3\text{H}_6)(\text{CN})_2(\text{CO})_4]$, (d) $\text{Fe}_2(\text{S}_2\text{C}_3\text{H}_6)(\text{CO})_6$ and $(\text{Et}_4\text{N})[\text{Fe}_2(\text{S}_2\text{C}_3\text{H}_6)(\text{CN})(\text{CO})_5]$, (e) product of the reaction of $\text{Fe}_2(\text{S}_2\text{C}_3\text{H}_6)(\text{CO})_6$, $(\text{Et}_4\text{N})[\text{Fe}_2(\text{S}_2\text{C}_3\text{H}_6)(\text{CN})(\text{CO})_5]$, and 2 equiv of Et_4NCN .

Conclusions

A range of derivatives of the type $[\text{Fe}_2(\text{SR})_2(\text{CN})_2(\text{CO})_4]^{2-}$ can be prepared by CN^- -for-CO substitution reactions. These syntheses occur for alkyl- and arylthiolato derivatives and for alkylidithiolates. The products are stable and have been fully characterized by X-ray diffraction for three derivatives ($\text{S}_2\text{C}_2\text{H}_4$, $\text{S}_2\text{C}_3\text{H}_6$, and $(\text{SCH}_2)_2\text{NMe}^{12}$). IR spectra of the dicyanides and the reduced form of the enzymes^{9,22} are similar (Figure 8), which is important because ν_{CO} bands are quite sensitive to the electron density at the metal center. For example, Liaw et al. have shown that ferrous thiolato carbonyls have significantly higher frequency ν_{CO} bands. In other words, our data suggest that the reduced enzyme features Fe(I) centers.

Crystallographic studies and IR data indicate that the dicyanide derivatives are electronically very similar for a variety of dithiolates. The variation among the solid-state structures implies that steric or crystal packing forces control the stereochemistry of the CO, CN^- , and PMe_3 ligands, especially considering the fluxionality of these ligands in solution. Independent of any electronic role, the dithiolate could have a functional role. It has recently been suggested⁷ that the Fe atoms are bridged by $\text{SCH}_2\text{NHCH}_2\text{S}$ (or N-protonated derivatives thereof) where the amine base participates as a hydrogen relay agent in the heterolytic activation and formation of H_2 ligands.

From the synthetic perspective, the unusual aspect of the dicyanides is their ready formation even with substoichiometric amounts of cyanide, that is, addition of 1 equiv of Et_4NCN to a solution of $\text{Fe}_2(\text{SR})_2(\text{CO})_6$ gives primarily $[\text{Fe}_2(\text{SR})_2(\text{CN})_2(\text{CO})_4]^{2-}$. Competition experiments demonstrate that hexacarbonyl $\text{Fe}_2(\text{S}_2\text{C}_3\text{H}_6)(\text{CO})_6$ reacts with cyanide more rapidly than does monocyanide $[\text{Fe}_2(\text{S}_2\text{C}_3\text{H}_6)(\text{CN})(\text{CO})_5]^-$.

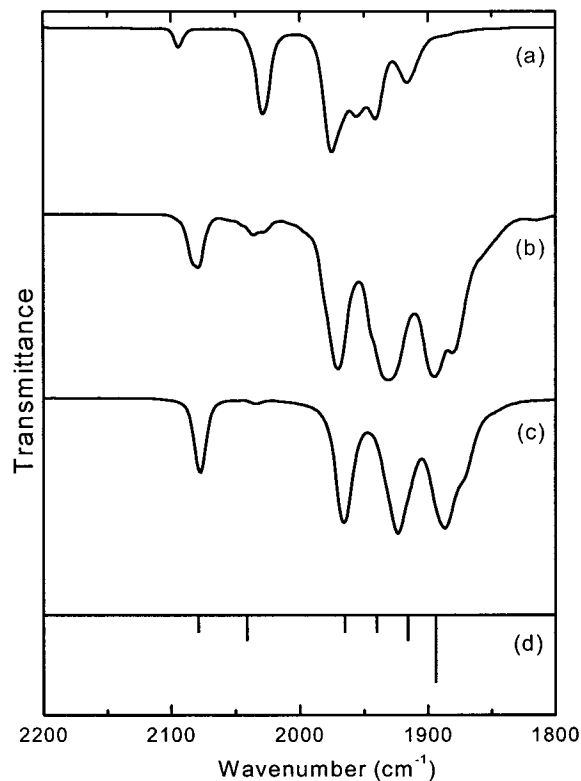


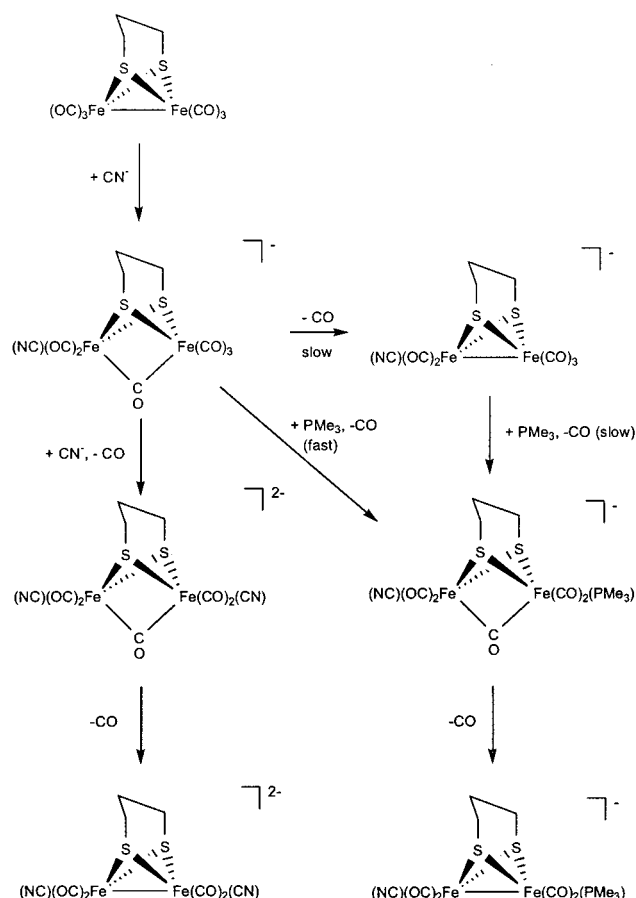
Figure 8. IR spectra of model compounds (a) $(\text{NEt}_4)[\text{Fe}_2(\text{S}_2\text{C}_3\text{H}_6)(\text{CN})(\text{CO})_5]$ (5), (b) $(\text{Et}_4\text{N})[\text{Fe}_2(\text{S}_2\text{C}_3\text{H}_6)(\text{CN})(\text{CO})_4(\text{PMe}_3)]$ (7), (c) $(\text{Et}_4\text{N})_2[\text{Fe}_2(\text{S}_2\text{C}_2\text{H}_4)(\text{CN})_2(\text{CO})_4]$ (3) and (d) the reduced active enzyme from *D. desulfuricans*.^{9,22} Spectra a and b were obtained on THF solutions, and spectrum c was obtained on a MeCN solution.

An associative substitution mechanism is particularly interesting because it implies an $\text{Fe}_2(\text{SR})_2\text{L}_7$ intermediate, the coordination number for which matches that for the Fe-only H_2 -ase enzyme (in both the CO-inhibited form and the resting form which has a terminal water ligand⁹) in the *Clostridium pasteurianum* as well as in the *Desulfovibrio desulfuricans* Fe-only H_2 -ase enzyme (where it is suggested that a terminal hydride or H_2 occupies one coordination site⁷). The observation of associative kinetics by Darensbourg et al.²⁶ is consistent with earlier studies on the substitution of $\text{Fe}_2(\text{SMe})_2(\text{CO})_6$ by phosphine ligands.^{16,27} What is surprising is the elusiveness of $[\text{Fe}_2(\text{S}_2\text{C}_3\text{H}_6)(\text{CN})(\text{CO})_5]^-$ from the reaction of $\text{Fe}_2(\text{SR})_2(\text{CO})_6$ with 1 equiv of cyanide, which obviously indicates that substitution by the second cyanide is competitive with the binding of the first cyanide. Normally in CO substitution reactions, the second CO is replaced far more slowly than the first. For example, the reaction of $\text{Cp}_2\text{Mo}_2(\text{SMe})_2(\text{CO})_2$ with CN^- affords only the monocyanide $[\text{Cp}_2\text{Mo}_2(\text{SMe})_2(\text{CN})(\text{CO})]^-$.³⁴ The anomalously high disubstitution rate is consistent with our finding that mixtures of CN^- and PMe_3 effect rapid conversion of the hexacarbonyl to $[\text{Fe}_2(\text{S}_2\text{C}_3\text{H}_6)(\text{CN})(\text{CO})_4(\text{PMe}_3)]^-$. We propose that the unusual reactivity of $\text{Fe}_2(\text{S}_2\text{C}_3\text{H}_6)(\text{CO})_6$ toward cyanide and a second donor ligand (CN^- or PR_3) is due to the stabilization of the electrophilic adduct $[\text{Fe}_2(\text{S}_2\text{C}_3\text{H}_6)(\text{CN})(\mu\text{-CO})(\text{CO})_5]^-$ (Scheme 4). Not only does this mechanism accord with the associative kinetics, it also accommodates the detection of a $\mu\text{-CO}$ intermediate by Pickett et al.³⁵ (Scheme 4). The stabilization of $[\text{Fe}_2(\text{S}_2\text{C}_3\text{H}_6)(\text{CN})(\mu\text{-CO})(\text{CO})_5]^-$ may be attributed to the small size and high basicity of cyanide,

(34) Absasq, M.-L.; Pétillon, F. Y.; Talarmin, J. J. *Chem. Soc., Chem. Commun.* **1994**, 2191–2192.

(35) Razavet, M.; Davies, S. C.; Hughes, D. L.; Pickett, C. J. *Chem. Commun.* **2001**, 847–848.

Scheme 4



which is well-known to stabilize high coordination numbers,³⁶ while the electrophilicity of the $\text{Fe}(\mu\text{-CO})(\text{CO})_3$ center can be attributed to its coordination to four CO ligands and the localization of the negative charge on the $\text{Fe}(\text{CN})(\text{CO})_2$ center due to the absence of an Fe–Fe bond. Otherwise, compounds of the type $[\text{Fe}_2(\mu\text{-L})(\text{SR})_2(\text{CO})_4\text{L}'_2]^{2-}$ are best known for $\text{L} = \text{H}$.^{14,25b,37} Finally, the redox properties of the dicyanides are pertinent because the hydrogenase enzymes are redox-active. For the series $[\text{Fe}_2(\text{S}_2\text{C}_3\text{H}_6)(\text{L})_2(\text{CO})_4]$ ($\text{L} = \text{CO}$, CNMe , PMe_3 , and CN^-), the dicyanide is the most reducing. Thus, while one could describe cyanide as “Nature’s trimethyl phosphine”, it is in fact a much more strongly donating ligand and, importantly, a ligand whose donor properties can be modulated by the pH of its environment.³⁸

Experimental Section

General Procedures. Organosulfur and organophosphorus compounds, Et_4NCN , and $\text{Fe}(\text{CO})_5$ were obtained from Aldrich and used without further purification. Solvents were purified by degassing with a nitrogen purge and were dispensed through two 1-m long columns of active alumina. Reactions were carried out under an atmosphere of purified nitrogen using either standard Schlenk techniques or in an inert atmosphere glovebox.

The following compounds were prepared by minor variations of literature methods: $\text{Fe}_2(\text{S}_2\text{C}_2\text{H}_4)(\text{CO})_6$, $\text{Fe}_2(\text{S}_2\text{C}_3\text{H}_6)(\text{CO})_6$ (**1**),²¹ Fe_2 –

$(\text{SCH}_3)_2(\text{CO})_6$,³ $\text{Fe}_2(\text{S}-4\text{-C}_6\text{H}_4\text{CH}_3)_2(\text{CO})_6$,³⁹ $\text{Fe}_2(\text{S}_2\text{CH}_2)(\text{CO})_6$,¹⁷ $\text{Fe}_2(\text{S}-2,2\text{-C}_{10}\text{H}_{14})(\text{CO})_6$,¹⁸ and $\text{Fe}_2(\text{S}-t\text{-Bu})_2(\text{CO})_6$.⁴⁰ The procedure is as follows: 1.5 g of $\text{Fe}_3\text{CO}_{12}$ was suspended in 100 mL of toluene followed by the addition of 1 equiv of the disulfide ($\text{R} = \text{Me}$, $t\text{-Bu}$) or dithiol ($\text{R} = (\text{CH}_2)_2$, $(\text{CH}_2)_3$) or 2 equiv of monothiol ($\text{R} = \text{S}-4\text{-C}_6\text{H}_4\text{CH}_3$). The reaction mixture was stirred at 70 °C until its color changed from deep green to dark red. The reaction mixture was allowed to cool to room temperature and filtered. The red filtrate was evaporated to dryness under vacuum, and the residue was extracted with 3 × 10 mL of hexanes. The combined extracts were reduced under vacuum to ~5 mL and cooled to –20 °C to give red crystals of $\text{Fe}_2(\text{SR})_2(\text{CO})_6$. Yield: 75–85%. $\text{Fe}_2(\text{S}_2\text{C}_3\text{H}_6)(\text{CO})_4(\text{PMe}_3)_2$ was prepared in the usual way by the thermal reaction of $\text{Fe}_2(\text{S}_2\text{C}_3\text{H}_6)(\text{CO})_6$ and PMe_3 .^{33a}

Electrochemistry. The cyclic voltammetry experiments were conducted in a ~10-mL one-compartment glass cell. The counter electrode was a Pt wire, the reference electrode a Ag/AgCl , KCl saturated electrode, and the working electrode either a glassy carbon or a Pt disk (3 or 2 mm in diameter, respectively). The concentration in electroactive compound was ~4 mM. Controlled-potential electrolysis was performed at a Pt working electrode in a two-compartment cell.

Crystallography. Crystals were mounted to a thin glass fiber using oil (Paratone-N, Exxon). Data were filtered to remove statistical outliers. The integration software (SAINT) was used to test for crystal decay as a bilinear function of X-ray exposure time and $\sin(\theta)$. Data were collected at 198 K on a Siemens CCD diffractometer. Crystal and refinement details are given in Table 2. The structures were solved using SHELXTL by direct methods; correct atomic positions were deduced from an E map or by an unweighted difference Fourier synthesis. H atom U's were assigned as 1.2 times the U_{eq} s of adjacent C atoms. Non-H atoms were refined with anisotropic thermal coefficients. Successful convergence of the full-matrix least-squares refinement of F^2 was indicated by the maximum shift/error for the last cycle.

(Et_4N) $_2[\text{Fe}_2(\text{S}_2\text{C}_3\text{H}_6)(\text{CN})_2(\text{CO})_4]$ (2**).** A solution of 1.00 g (2.59 mmol) of $\text{Fe}_2(\text{S}_2\text{C}_3\text{H}_6)(\text{CO})_6$ in 20 mL of MeCN at 0 °C was treated with a solution of 0.80 g (5.12 mmol) of Et_4NCN in 10 mL of MeCN, and then the mixture was allowed to warm to room temperature. After 1 h further, the resulting dark red solution was evaporated to dryness. The solid residue was washed with 15 mL of hexanes. Yield: 1.56 g (94%). Anal. Calcd for $\text{C}_{25}\text{H}_{46}\text{Fe}_2\text{N}_4\text{O}_4\text{S}_2$: C, 46.74; H, 7.22; N, 8.72; S, 9.98; Fe, 17.38. Found: C, 46.75; H, 7.21; N, 9.07; S, 9.63; Fe, 17.20. ^1H NMR (400 MHz, CD_3CN): δ 3.18 (q, 16H, NCH_2CH_3), 1.85 (t, 4 H, SCH_2), 1.67 (m, 2H, $\text{CH}_2\text{CH}_2\text{CH}_2$), 1.21 (t, 24H, NCH_2CH_3). IR (KBr): $\nu_{\text{CN}} = 2078, 2029$; $\nu_{\text{CO}} = 1961, 1917, 1880, 1867\text{ cm}^{-1}$.

(Et_4N) $_2[\text{Fe}_2(\text{S}_2\text{C}_3\text{H}_6)(^{13}\text{CN})_2(\text{CO})_4]$ (50% Enriched) (2a**).** A solution of 0.20 g (1.30 mmol) of Et_4NCN and 0.08 g (1.30 mmol) of K^{13}CN in 10 mL of CH_3OH was stirred for 10 h. The solvent was removed under vacuum, and the resulting solid was slurried in 5 mL of MeCN. The suspension was filtered into a solution of 0.25 g (0.65 mmol) of $\text{Fe}_2(\text{S}_2\text{C}_3\text{H}_6)(\text{CO})_6$ in 20 mL of MeCN at 0 °C. The reaction mixture was allowed to warm to room temperature. After an additional 1 h, the resulting dark red solution was evaporated to dryness under vacuum. The residue was washed with 15 mL of hexanes. Yield: 0.19 g (46%). ^1H NMR (500 MHz, CD_3OD): δ 3.22 (q, 16H, NCH_2CH_3), 1.84 (t, 4 H, SCH_2), 1.66 (m, 2H, $\text{CH}_2\text{CH}_2\text{CH}_2$), 1.22 (t, 24H, NCH_2CH_3). ^{13}C NMR (500 MHz, CD_3OD): δ 219.5 (s, 4C, FeCO), 164.5 (s, 2C, FeCN), 53.5 (s, 8C, NCH_2CH_3), 31.6 (s, 2C, SCH_2), 23.9 (s, 1C, $\text{CH}_2\text{CH}_2\text{CH}_2$), 7.8 (s, 8C, NCH_2CH_3). IR (CH_2Cl_2): $\nu_{\text{CN}} = 2071, 2031$; $\nu_{\text{CO}} = 1964, 1924, 1884\text{ cm}^{-1}$.

(Et_4N) $_2[\text{Fe}_2(\text{SCH}_3)_2(\text{CN})_2(\text{CO})_4]$ (3**).** A solution of 0.41 g (1.11 mmol) of $\text{Fe}_2(\text{SCH}_3)_2(\text{CO})_6$ in 20 mL of MeCN at 0 °C was treated with a solution of 0.35 g (2.22 mmol) of Et_4NCN in 5 mL of MeCN. The reaction mixture was allowed to come to room temperature. After 1 h further, the resulting dark red solution was evaporated to dryness under vacuum. The residual solid was washed with 15 mL of hexanes. Yield: 0.58 g (83%). Anal. Calcd for $\text{C}_{24}\text{H}_{46}\text{Fe}_2\text{N}_4\text{O}_4\text{S}_2$: C, 45.72; H, 7.35; N, 8.89; S, 10.17; Fe, 17.72. Found: C, 45.97; H, 7.33; N, 8.98; S, 10.34; Fe, 17.59. ^1H NMR (400 MHz, CD_3CN): δ 3.21 (q, 16H, NCH_2CH_3), 1.83 (s, 3H, 73% *a,e* isomer, SCH_3), 1.74 (s, 6H, 27% *e,e*

(36) Sharpe, A. G. *The Chemistry of Cyano Complexes of the Transition Metals*; Academic Press: London, 1976.

(37) (a) Fauvel, K.; Mathieu, R.; Poilblanc, R. *Inorg. Chem.* **1976**, *15*, 976–978. (b) Savariault, J.-J.; Bonnet, R.; Mathieu, R.; Galy, J. C. *R. Acad. Sci., Ser. IIC: Chim.* **1977**, 663–667. (c) Zhao, X.; Georgakaki, I. P.; Miller, M. L.; Yarbrough, J. C.; Darensbourg, M. Y. *J. Am. Chem. Soc.* **2001**, *123*, 9710–9711.

(38) For example, see: Datta, D.; Mascharak, P. K.; Chakravorty, A. *Inorg. Chem.* **1981**, *20*, 1673–1679.

(39) Treichel, P. M.; Crane, R. A.; Matthews, R.; Bonnin, K. R.; Powell, D. J. *Organomet. Chem.* **1991**, *402*, 233–248.

(40) King, R. B.; Bisnette, M. B. *Inorg. Chem.* **1965**, *4*, 482–485.

Table 2. Details of Data Collection and Structure Refinement for **3**, **5**, **6c**, and **7**

	3	5	6c	7
chemical formula	C ₂₄ H ₄₄ Fe ₂ N ₄ O ₄ S ₂	C ₁₇ H ₂₆ Fe ₂ N ₂ O ₅ S ₂ ·0.9THF	C ₂₆ H ₄₂ Fe ₂ KNO ₁₁ S ₂	C ₃₈ H ₇₀ Fe ₄ N ₄ O ₈ P ₂ S ₄
temperature (K)	193(2)	193(2)	193.2	193(2)
crystal size (mm)	0.01 × 0.48 × 0.80	0.36 × 0.18 × 0.08	0.03 × 0.03 × 0.76	0.04 × 0.12 × 0.22
space group	<i>P</i> $\bar{1}$	<i>P</i> $\bar{1}$	<i>P</i> ₂ / <i>c</i>	<i>P</i> ₂ / <i>c</i>
<i>a</i> (Å)	7.7580(14)	7.6421(11)	20.563(2)	11.1882(16)
<i>b</i> (Å)	10.0251(18)	10.4061(14)	8.7120(9)	32.862(5)
<i>c</i> (Å)	19.747(4)	16.846(2)	20.342(2)	14.280(2)
α (deg)	90.774(3)	102.859(3)	90	90
β (deg)	98.760(4)	91.197(14)	103.588(2)	95.300(3)
γ (deg)	96.712(4)	99.024	90	90
<i>V</i> (Å ³)	1506.7(5)	1287.7(3)	3542.2(6)	5228.0(13)
<i>Z</i>	2	2	4	4
<i>D</i> calcd (Mg m ⁻³)	1.385	1.492	1.424	1.356
μ (Mo K α , mm ⁻¹)	0.710 73	0.710 73	0.710 73	0.710 73
max/min transn	0.9942/0.6117	1.0000/0.7937	0.9671/0.8392	0.9967/0.7932
reflms measured/independent	7992/5237	11 956/6015	15 375/4950	31 219/9225
data/restraints/parameters	5237/40/361	6015/8/350	4943/739/605	9225/0/555
GOF	0.942	1.044	0.787	0.878
<i>R</i> _{int}	0.0680	0.0277	0.1760	0.1108
<i>R</i> ₁ [<i>I</i> > 2 σ] (all data) ^a	0.0616 (0.1250)	0.0380 (0.0529)	0.0499 (0.0609)	0.0490 (0.0808)
<i>R</i> _w [<i>I</i> > 2 σ] (all data) ^b	0.1361 (0.1608)	0.1061 (0.1135)	0.1887 (0.0808)	0.1352 (0.0970)
max peak/hole (e ⁻ /Å ³)	0.617/-0.669	0.810/-0.376	0.350/-0.381	0.603/-0.396

^a $R = \sum ||F_o| - |F_c|| / \sum |F_o|$. ^b $R_w = \{ \sum [w(|F_o| - |F_c|)^2] / \sum [wF_o^2] \}^{1/2}$, where $w = 1/\sigma^2(F_o)$.

Table 3. *a,e* vs *e,e* Isomer Ratios in Fe₂(SR)₂(CO)₆ and Derivatives in MeCN Solution Determined by ¹H NMR Spectroscopy

compound	<i>a,e/e,e</i> ratio
Fe ₂ (SMe) ₂ (CO) ₆	67/33
[Fe ₂ (SMe) ₂ (CN) ₂ (CO) ₄] ²⁻	73/27
Fe ₂ (S- <i>t</i> -Bu) ₂ (CO) ₆	81/19
[Fe ₂ (S- <i>t</i> -Bu) ₂ (CN)(CO) ₅] ⁻	78/22
[Fe ₂ (S- <i>t</i> -Bu) ₂ (CN) ₂ (CO) ₄] ²⁻	70/30
Fe ₂ (SC ₆ H ₅ Me) ₂ (CO) ₆	20/80
[Fe ₂ (SC ₆ H ₅ Me) ₂ (CN) ₂ (CO) ₄] ²⁻	93/7

isomer, SCH₃), 1.21 (t, 24H, NCH₂CH₃), 1.20 (s, 3H, 73% *a,e* isomer, SCH₃) (Table 3). IR (KBr): $\nu_{\text{CN}} = 2072, 2037$; $\nu_{\text{CO}} = 1961, 1913, 1879 \text{ cm}^{-1}$.

(Et₄N)₂[Fe₂(S-4-C₆H₄Me)₂(CN)₂(CO)₄]. A solution of 0.53 g (2.59 mmol) of Fe₂(S-4-C₆H₄Me)₂(CO)₆ in 10 mL of MeCN at 0 °C was treated with a solution of 0.31 g (2.00 mmol) of Et₄NCN in 5 mL of MeCN. The reaction mixture was allowed to come to room temperature. After an additional 1 h, the resulting dark red solution was evaporated to dryness under vacuum. The remaining red solid was washed with 3 × 5 mL of hexanes. Yield: 0.71 g (91%). Anal. Calcd for C₃₆H₅₄Fe₂N₄O₄S₂: C, 55.25; H, 6.95; N, 7.16; S, 8.19; Fe, 14.27. Found: C, 54.23; H, 6.52; N, 6.49; S, 8.45; Fe, 14.33. ¹H NMR (400 MHz, CD₃-CN): δ 7.51–6.76 (m, 8H, C₆H₄), 3.16 (q, 16H, NCH₂CH₃), 2.20 (s, 3H, 93.4% *a,e* isomer, C₆H₄CH₃), 2.18 (s, 6H, 6.6% *e,e* isomer, C₆H₄CH₃), 2.17 (s, 3H, 93.4% *a,e* isomer, C₆H₄CH₃), 1.19 (t, 24H, NCH₂CH₃) (Table 3). IR (KBr): $\nu_{\text{CN}} = 2092, 2078, 2033$; $\nu_{\text{CO}} = 1976, 1931, 1900 \text{ cm}^{-1}$.

(Et₄N)₂[Fe₂(S₂C₂H₄)(CN)₂(CO)₄] (**3**). A solution of 1.00 g (2.68 mmol) of Fe₂(S₂C₂H₄)(CO)₆ in 10 mL of MeCN was treated with a solution of 0.84 g (5.36 mmol) of Et₄NCN in 5 mL of MeCN. The reaction proceeded as for the propanedithiolate. After 1 h, the resulting dark red solution was evaporated to dryness under vacuum. The residue was washed with 5 mL of Et₂O and recrystallized by dissolution in MeCN, followed by dilution with Et₂O. Yield: 1.37 g (82%). Single crystals were grown from a concentrated MeCN solution that was layered with Et₂O. Anal. Calcd for C₂₄H₄₄Fe₂N₄O₄S₂: C, 45.87; H, 7.06; N, 8.91; Fe, 17.77. Found: C, 45.78; H, 6.91; N, 8.90; Fe, 17.95. ¹H NMR (500 MHz, CD₃OD): δ 3.28 (q, 16H, NCH₂CH₃), 1.96 (s, 4 H, SCH₂), 1.21 (t, 24H, NCH₂CH₃). IR (MeCN): $\nu_{\text{CN}} = 2077, 2033$ (w); $\nu_{\text{CO}} = 1965, 1924, 1886, 1870 \text{ cm}^{-1}$.

(Et₄N)₂[Fe₂(S₂C₂H₄)(¹³CN)₂(CO)₄] (**50% Enriched**) (**3a**). A solution of 0.20 g (1.30 mmol) of Et₄NCN and 0.08 g (1.30 mmol) of K¹³CN in 15 mL of CH₃OH was stirred for 30 min. The solvent was removed

under vacuum, and the resulting solid was extracted into 5 mL of MeCN. The suspension was filtered into a solution of 0.24 g (0.65 mmol) of Fe₂(S₂C₂H₄)(CO)₆ in 10 mL of MeCN. The reaction mixture was stirred for 1 h further. The resulting dark red solution was evaporated to dryness under vacuum. The residue was washed with 15 mL of hexanes and recrystallized by extraction into ~5 mL of MeCN followed by the addition of Et₂O. Yield: 0.35 g (78%). ¹H NMR (500 MHz, CD₃OD, 25 °C): δ 3.28 (q, 16H, NCH₂CH₃), 1.96 (2, 4 H, SCH₂), 1.21 (t, 24H, NCH₂CH₃). ¹³C NMR (500 MHz, CD₃OD): δ 219.5 (s, 4C, FeCO), 164.5 (s, 2C, FeCN), 53.5 (s, 8C, NCH₂CH₃), 31.6 (s, 2C, SCH₂), 23.9 (s, 1C, CH₂CH₂CH₃), 7.8 (s, 8C, NCH₂CH₃). IR (MeCN): $\nu_{\text{CN}} = 2077, 2033$ ($\nu_{\text{CN}} = 2033$ (s)); $\nu_{\text{CO}} = 1965, 1924, 1886, 1870 \text{ cm}^{-1}$.

Fe₂(S₂C₃H₆)(CO)₅(CNMe) and Fe₂(S₂C₃H₆)(CO)₄(CNMe)₂ (**4**). A solution of 0.500 g (1.30 mmol) of **1** in 60 mL of MeCN was treated with 250 μ L (4.60 mmol) of CNMe, followed by the addition of 0.290 g (2.61 mmol) of Me₃NO in 20 mL of MeCN. After 5 h, TLC showed the reaction was complete. The dark red solution was filtered and evaporated to dryness under vacuum. The residue was extracted into 5 mL of toluene and passed through a 3 cm × 20 cm column of silica gel, eluting with hexane–toluene 3:1. Two bands were observed: the first orange band (Fe₂(S₂C₃H₆)(CO)₅(CNMe); IR (hexane): $\nu_{\text{CN}} = 2185$; $\nu_{\text{CO}} = 2044, 2003, 1971 \text{ cm}^{-1}$) was collected with ~500 mL of eluant, and the second red band (**4**) with ~300 mL of toluene. Yield: 0.160 g (30%). ¹H NMR (500 MHz, C₆D₆): δ 1.94 (s, 6H, NCH₃), 1.73 and 1.40 (4 and 2H, S(CH₂)₃S). IR (MeCN): $\nu_{\text{CN}} = 2170$; $\nu_{\text{CO}} = 2020, 2000, 1967, 1936 \text{ cm}^{-1}$.

Generation of [Fe₂(S₂C₃H₆)(MeCN)(CO)₅]. A solution of 0.15 g (0.38 mmol) of Fe₂(S₂C₃H₆)(CO)₆ in 10 mL of MeCN was treated with a solution of 0.031 g (0.38 mmol) ONMe₃·2H₂O in 10 mL of MeCN. The solution immediately became dark purple. The IR spectrum of this solution showed $\nu_{\text{CO}} = 2051, 2040, 1991, 1964, 1933 \text{ cm}^{-1}$. Evaporation of the solution gave Fe₂(S₂C₃H₆)(CO)₆ and unidentified brown solids. If instead of evaporation the solution was treated with 0.50 g (1.9 mmol) PPh₃, the solution color lightened to red-orange, and the IR spectrum identified the main product as Fe₂(S₂C₃H₆)(CO)₅(PPh₃); $\nu_{\text{CO}} = 2045, 1985, 1932 \text{ cm}^{-1}$.²⁷

(Et₄N)[Fe₂(S₂C₃H₆)(CN)(CO)₅] (**5**). A solution of 0.35 g (0.87 mmol) of Fe₂(S₂C₃H₆)(CO)₆ in 10 mL of MeCN was treated with a solution of 0.097 g (0.87 mmol) ONMe₃·2H₂O in 10 mL of MeCN. The solution was then cooled to at -40 °C and treated with a solution of 0.137 g (0.87 mmol) of Et₄NCN in 10 mL of MeCN. The reaction mixture was allowed to warm to room temperature over the course of 2 h. The dark red solution was evaporated to dryness under vacuum. The resulting red oil was extracted into 10 mL of THF, and this extract

was filtered. The volume was reduced to approximately 1 mL, and the product was precipitated upon addition of 20 mL of hexanes and washed with 45 mL of hexanes, giving a red solid. Single crystals were grown from THF solution by overlaying with hexanes. Yield: 0.46 g (79%). Anal. Calcd for $C_{17}H_{26}Fe_2N_2O_5S_2$: C, 39.71; H, 5.10; N, 5.45, S, 12.47. Found: C, 39.43; H, 5.06; N, 5.43, S, 12.47. 1H NMR (500 MHz, CD_3CN): δ 3.16 (q, 8H, NCH_2CH_3), 2.18 and 1.77 (br, 6H, $S(CH_2)_3S$), 1.19 (t, 12H, NCH_2CH_3). IR (THF): ν_{CN} = 2094; ν_{CO} = 2029, 1974, 1955, 1941, 1917 cm^{-1} .

(Et₄N)[Fe₂(S-*t*-Bu)₂(CN)(CO)₅] (6a). A solution of 0.20 g (0.44 mmol) of $Fe_2(S-t-Bu)_2(CO)_6$ in 10 mL of MeCN at 0 °C was treated with a solution of 0.07 g (0.44 mmol) of Et₄NCN in 5 mL of MeCN. The reaction mixture was allowed to warm to room temperature. After 24 h further, the resulting dark red solution was evaporated to dryness under vacuum. The remaining solid was washed with 15 mL of hexanes. Yield: 0.22 g (86%). Anal. Calcd for $C_{22}H_{38}Fe_2N_2O_5S_2$: C, 45.06; H, 6.53; N, 4.78; Fe, 19.05. Found: C, 44.44; H, 6.64; N, 5.14; Fe, 19.45. 1H NMR (400 MHz, CD_3CN): δ 3.13 (q, 8H, NCH_2CH_3), 1.32 (s, 18H, 21.9% *e,e* isomer, $SC(CH_3)_3$), 1.28 (s, 9H, 79% *a,e* isomer, $SC(CH_3)_3$), 1.23 (s, 9H, % *a,e* isomer, $SC(CH_3)_3$), 1.18 (t, 12H, NCH_2CH_3) (Table 3). IR (KBr): ν_{CN} = 2084; ν_{CO} = 2019, 1965, 1950, 1926, 1905 cm^{-1} . ESI-MS: m/z 456.1 (M^-), 428.1 ($M^- - CO$), 400.1 ($M^- - 2CO$), 372.2 ($M^- - 3CO$).

Ph₄PCN·H₂O. A solution of 1.55 g (23.80 mmol) of KCN in 10 mL of CH_3OH was treated dropwise with a solution of 6.44 g (15.36 mmol) of PPh₄Br in 10 mL of CH_3OH . The resulting suspension was evaporated to dryness, and the residue was extracted with 20 mL of MeCN. The extract was concentrated and stored at -32 °C to give colorless crystals. Yield: 2.50 g (42%). The water of crystallization can be removed by vacuum-drying for 24 h. Anal. Calcd for $C_{25}H_{22}NOP$: C, 78.31; H, 5.78; N, 3.65. Found: C, 78.19; H, 5.40; N, 3.17. IR (KBr): ν_{CN} = 2069 cm^{-1} .

(Ph₄P)[Fe₂(S-*t*-Bu)₂(CN)(CO)₅] (6b). A solution of 0.20 g (0.44 mmol) of $Fe_2(S-t-Bu)_2(CO)_6$ in 10 mL of MeCN at 0 °C was treated with a solution of 0.17 g (0.44 mmol) of Ph₄PCN·H₂O in 5 mL of MeCN. The reaction mixture was allowed to come to room temperature and stir for 24 h. The resulting dark red solution was evaporated to dryness under vacuum. The remaining solid was washed with 25 mL of hexanes. Yield: 0.14 g (40%). Anal. Calcd for $C_{38}H_{38}Fe_2NO_5PS_2$: C, 57.37; H, 4.81; N, 1.76; Fe, 14.04. Found: C, 57.57; H, 4.74; N, 1.55; Fe, 12.83. 1H NMR (400 MHz, CD_3CN): δ 7.94–7.64 (m, 20H, $P(C_6H_5)_4$), 1.31 (s, 18H, *e,e* isomer, $SC(CH_3)_3$), 1.28 (s, 9H, *e,a* isomer, $SC(CH_3)_3$), 1.23 (s, 9H, *a,e* isomer, $SC(CH_3)_3$) (Table 3). IR (KBr): ν_{CN} = 2086; ν_{CO} = 2023, 1969, 1939 cm^{-1} .

[K(18-crown-6)][Fe₂(S-*t*-Bu)₂(CN)(CO)₅] (6c). A solution of 0.10 g (0.22 mmol) of $Fe_2(S-t-Bu)_2(CO)_6$ in 10 mL of THF was treated with a solution of 0.01 g (0.22 mmol) of KCN and 0.06 g (0.23 mmol) of 18-crown-6 in 15 mL of a 2:1 mixture of MeCN and CH_3OH . The

reaction mixture was stirred for 120 h. The resulting dark red solution was evaporated to dryness under vacuum. The solid residue was washed with 15 mL of hexanes and recrystallized from THF by the addition of Et₂O. Single crystals of **11c** were obtained by layering a concentrated THF solution with Et₂O. 1H NMR (400 MHz, CD_3CN): δ 3.56 (s, 24H, OCH_2), 1.32 (s, 18H, 22% *e,e* isomer, $SC(CH_3)_3$), 1.28 (s, 9H, 77% *e,a* isomer, $SC(CH_3)_3$), 1.23 (s, 9H, 77% *a,e* isomer, $SC(CH_3)_3$) (Table 3). IR (KBr): ν_{CN} = 2087; ν_{CO} = 2020, 1972, 1929 cm^{-1} .

(Et₄N)[Fe₂(S₂C₃H₆)(CN)(CO)₄(PMe₃)] (7). A solution of 0.40 g (1.0 mmol) of $Fe_2(S_2C_3H_6)(CO)_6$ in 10 mL of MeCN at -40 °C was treated with a solution of 0.4 mL (4.0 mmol) of PMe₃ in 10 mL of MeCN followed by a solution of 0.15 g (0.95 mmol) of Et₄NCN in 5 mL of MeCN. The reaction mixture was warmed to -10 °C. After 30 min, the IR spectrum showed that all starting material had been consumed. The resulting dark red-purple solution was evaporated to dryness under vacuum. The red oil was extracted with 10 mL of THF and filtered. The volume was reduced under vacuum to ~5 mL, and the product was precipitated with 30 mL of pentane as an oil. The red oil was washed with an additional 3 × 30 mL of pentane, giving a solid. Single crystals were grown from toluene/hexanes at -20 °C. Yield: 0.50 g (92%). Anal. Calcd for $C_{19}H_{35}Fe_2N_2O_4PS_2$: C, 40.59; H, 6.29; N, 4.98. Found: C, 40.65; H, 6.34; N, 4.94. 1H NMR (500 MHz, C_6D_6): δ 2.79 (q, 8H, NCH_2CH_3), 2.17 and 2.08 (br, 4H, SCH_2), 1.89 and 1.68 (br, 2H, $CH_2CH_2CH_6$), 1.36 (d, 9H, CH_3), 0.87 (t, 12H, NCH_2CH_3). ^{31}P NMR (500 MHz, C_6D_6): δ 28.7 (s). IR (THF): ν_{CN} = 2078, 2036; ν_{CO} = 1971, 1931, 1895, 1880 cm^{-1} . FAB-MS: M^- 431.8 m/z .

Reaction of (Et₄N)[Fe₂(S₂C₃H₆)(CN)(CO)₅] (5) and Fe₂(S₂C₃H₆)(CO)₆ (1) with 2 equiv of Et₄NCN. A solution of 0.75 g (0.15 mmol) of (Et₄N)[Fe₂(S₂C₃H₆)(CN)(CO)₅] and 0.56 g (0.15 mmol) of Fe₂(S₂C₃H₆)(CO)₆ in 20 mL of MeCN at -40 °C was treated with a solution of 0.46 g (0.31 mmol) of Et₄NCN in 10 mL of MeCN. The reaction mixture was allowed to warm to room temperature over the course of 30 min. IR spectra were obtained after the solution had been warmed to room temperature, after 1 h, and after 3 h. The IR spectrum showed that all Fe₂(S₂C₃H₆)(CO)₆ had been consumed after 3 h. IR (MeCN): ν_{CN} = 2092, 2075, 2030; ν_{CO} = 1975, 1963, 1921, 1883 cm^{-1} (see Figure 7).

Acknowledgment. This research was supported by NIH and DOE. F.G. thanks the CNRS (France) for a leave of absence. S. Contakes is thanked for assistance and advice.

Supporting Information Available: Crystallographic information and IR data (PDF). This material is available free of charge via the Internet at <http://pubs.acs.org>.

JA016071V